Industrial Crops & Products 171 (2021) 113984

Contents lists available at ScienceDirect

Industrial Crops & Products

journal homepage: www.elsevier.com/locate/indcrop

On the production and release of *Hedychium coronarium* essential oil from nanoformulations

Caroline F. da Silva , Rafaela R. Petró , Rafael N. Almeida *, Eduardo Cassel , Rubem M.F. Vargas

Unit Operations Lab, Polytechnic School, Pontifical Catholic University of Rio Grande do Sul, Av. Ipiranga 6681 - Prédio 30, Bloco F, Sala 208, Porto Alegre, Brazil

ARTICLE INFO

Keywords:
Nanocapsules
Nanoemulsion
Polycaprolactone
Steam distillation
Mathematical modeling

ABSTRACT

Biopolymers are usually used in encapsulation techniques to protect natural products from degradation. The essential oil of *Hedychium coronarium* presents a floral scent, which justifies its use in perfumes, in addition, its antimicrobial activity may contribute to its stability as natural protectant. Thus, this work aims to investigate the *Hedychium coronarium* essential oil extraction by steam distillation and to enhance the physicochemical stability of this essential oil through encapsulation in polycaprolactone, also preserving its odor properties. The employed nanoprecipitation process presented a 1:3 optimal polymer/oil ratio, which yielded an average particle diameter of 159 nm. The morphology was evaluated by field emission scanning electron microscopy (FESEM) and transmission electron microscopy (TEM), the essential oil encapsulation was confirmed by thermogravimetric analysis (TGA). The formulations pH remained stable for 90 days and the controlled release of the compounds was evaluated through antioxidant activity analysis. The release and diffusion of compounds from the formulations were evaluated over time and fitted with the Peppas equation.

1. Introduction

Hedychium coronarium, popularly known as butterfly ginger and white ginger lily, is an Asian native species, classified as an invader in South America. Volatile oils are found more abundantly in its rhizomes, presenting eucalyptol, β-pinene, α-pinene, and α-terpineol among its major components (dos Santos et al., 2010; Lechat-Vahirua et al., 1993; Ray et al., 2018a). The presence of eucalyptol, known to have an extensive biological activity (Caldas et al., 2015), and especially the presence of monoterpenes β-pinene and α-terpineol, gives support to the use of *H. coronarium* rhizomes in folk medicine. The essential oils are used in different formulations (detergents, soaps, cosmetics, and lotions) due to their pleasant fragrance and antimicrobial effect (Falcão et al., 2012; Ray et al., 2018a; Sakhanokho et al., 2013; Xavier et al., 2013). Among others, studies indicate strong antioxidant activity of leaf and rhizomes extracts (Hartati et al., 2014), and also activity against *Trichoderma* sp. and *Candida albicans* (Joy et al., 2007).

The sweet, spicy, and floral scents from the *H. coronarium* flower oil are attributed to linalool, methyl jasmonate, eugenol, cis-jasmone, β-ionone, and lactone (Ali et al., 2002; Omata et al., 1991). Headspace analysis of volatile flower compounds presents a composition of 35 % monoterpenic hydrocarbons, 34 % oxygenated monoterpenes, and 13 % sesquiterpene hydrocarbons. The major compounds are (E)-β-ocimene (29 %), linalool (19 %), and eucalyptol (15 %), which contribute to the floral scent (Chan and Wong, 2015). Due to their complexity, perfumes are classified qualitatively in olfactory families referring to the predominant fragrant notes, which can be associated with the headspace concentration (Teixeira et al., 2012).

In order to protect natural products from degradation, encapsulation techniques using polymeric particles have been widely investigated, providing many other advantages (Piorkowski and McClements, 2014) such as the controlled release of aromas and drugs, through techniques such as micro or nano-encapsulation in emulsions, the protection and modulation of the release of active constituents present in essential oils are currently being applied, transforming liquid and volatile products into solid or gel and enabling better absorption of hydrophilic and lipophilic constituents (El Asbahani et al., 2015; Castangia et al., 2015). The greatest limitations of the process are the losses caused by a heating or a vaporization step (Castangia et al., 2015; El Asbahani et al., 2015). Nanoprecipitation is a traditional technique, used for the nano-encapsulation of hydrophobic compounds, producing monodispersed nanoparticles. The different methods result in diverse physical-chemical characteristics, such as average droplet size, polydispersity index, and zeta potential, which, in turn, influence the formulation stability, the

* Corresponding author.
E-mail address: r.nolibos@edu.pucrs.br (R.N. Almeida).

https://doi.org/10.1016/j.indcrop.2021.113984
Received 20 April 2021; Received in revised form 11 August 2021; Accepted 23 August 2021
Available online 27 August 2021

Table 1
Formulations prepared for the *H. coronarium* essential oil nanoencapsulation.

Essential oil extraction pressure	Formulation	Polymer/ Oil	Polymer (mg)	Essential oil (mg)
	111	1:1	25	25
	112	1:2	25	50
1 bar	113	1:3	25	75
	114	1:4	25	100
	115	1:5	25	125
	211	1:1	25	25
	212	1:2	25	50
2 bar	213	1:3	25	75
	214	1:4	25	100
	215	1:5	25	125
	311	1:1	25	25
	312	1:2	25	50
3 bar	313	1:3	25	75
	314	1:4	25	100
	315	1:5	25	125
Polymer particle	PP	–	25	–

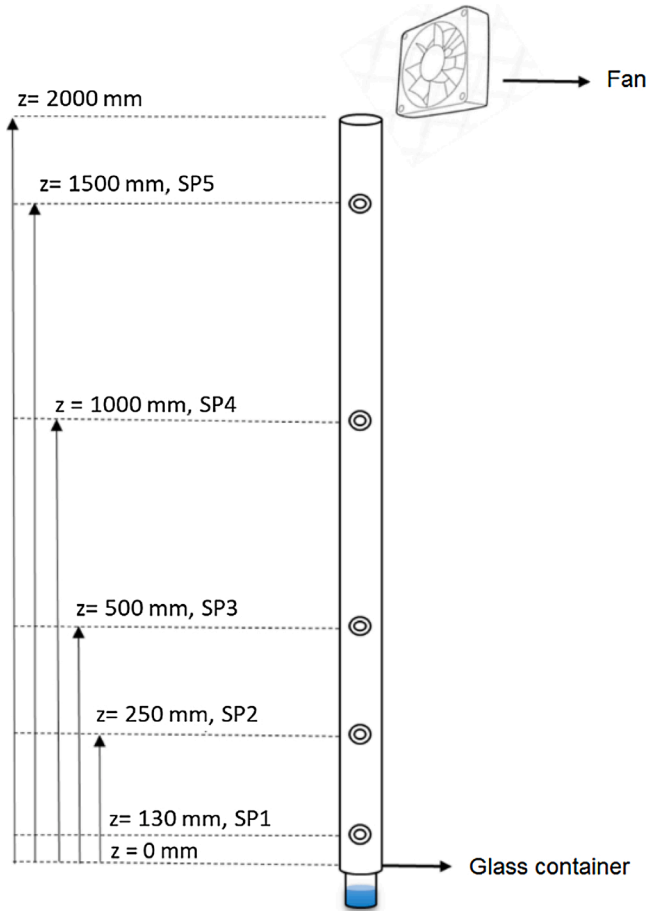

Fig. 1. Diffusion tube scheme.

Table 2
Extraction yield of *H. coronarium* oil using different absolute process pressures.

Pressure (bar)	ρ_{oil} (kg/m^3)	Yield (% kg $_{oil}$ / kg $_{rhizome}$)
1	866 ± 3.8	0.210 ± 0.023^a
2	855 ± 5.8	0.376 ± 0.060^b
3	930 ± 4.0	0.183 ± 0.024^a

Values with equal superscript in each column do not present significant difference ($p<0.05$).

system interactions with the skin, and the controlled release from the carriers (Beck et al., 2011; Ezhilarasi et al., 2013).

This work aims to investigate the complete nanoencapsulation process of the *Hedychium coronarium* essential oil, from its extraction until potential product performance. It was evaluated the optimal process conditions for the steam distillation, performing the mathematical modeling of the extraction and analyzing the essential oil chemical composition. The nanoparticles produced using the encapsulating agent polycaprolactone, a biodegradable and biocompatible polymer, widely used in various industrial applications, and the nanoemulsions were characterized. To the best our knowledge this is the first report on nanoparticle and nanoemulsion production of the *H. coronarium* essential oil and subsequent fragrance release investigation. The *H. coronarium* essential oil, its nanoemulsion, and its nanoparticles had their experimental diffusive profiles evaluated and the Peppas (1985) model was fitted.

2. Material and methods

2.1. Standard compounds and chemicals

Analytical standards of α-pinene (≥99 %), β-pinene (99 %), eucalyptol (≥99 %), β-caryophyllene (≥80 %), n-alkane series (C_8-C_{20}) and uranyl acetate (2% dilution) were obtained from Sigma Chemical Co. (St. Louis, MO, USA). All solvents (acetone, cyclohexane, methanol) used in the experiments were of analytical grade obtained from Merck, Germany. 2,2-diphenyl-1-picrylhydrazyl (DPPH) was obtained from Sigma. Span® 60 acquired from Merck, Spain and Tween 80 U.S.P. from Synth, Brazil. Polycaprolactone (PCL) procured from PURAC, Germany. Milli-Q® water from Merck IQ 7003/05/10/15 Water Purification Systems.

2.2. Plant material

The plant material was harvested in the city of Maquiné (29°41′48.5″S 50°10′07.0″W) in the state of Rio Grande do Sul, southern Brazil, during the flowering period in the first week of January (summer). Only the plant rhizomes were used, and these were cleaned, cut into cubes, and milled in an industrial blender. The material was conditioned at room temperature for a maximum period of one week in 100 g batches. The samples were analyzed for their moisture content in thermogravimetric scale (BEL Engineering), the specific mass was determined with a multipicnometer (Quantachrome) and the average thickness was characterized with a digital pachymeter Mitutoyo.

2.3. Steam distillation

The essential oil was obtained in a pilot steam distillation plant. The unit is previously described in detail by de Souza et al. (2020), basically the extraction unit consists of a boiler heated by an electric resistor for water vapor production with a volume of 20 L, an extraction chamber where the plant material is deposited with a capacity of 10 L, a heat exchanger, and a liquid-liquid separator where the oil, due to the difference in density, separates from the condensed water. The experiments were initially performed with different quantities, 0.5 kg, 1 kg, and 2 kg of the milled rhizome, to evaluate the influence of the bed geometry. Afterward, with the best configuration, extractions were performed at three different absolute pressures, 1 bar, 2 bar, and 3 bar, evaluating its effect on the process yield, as well as on the extraction kinetics and the essential oil composition. To construct the yield *versus* time curves, the experiments were carried out in triplicate, and the amount of essential oil extracted every 5 min was measured, starting from the first condensate droplet until no significant variation in the extracted oil volume.

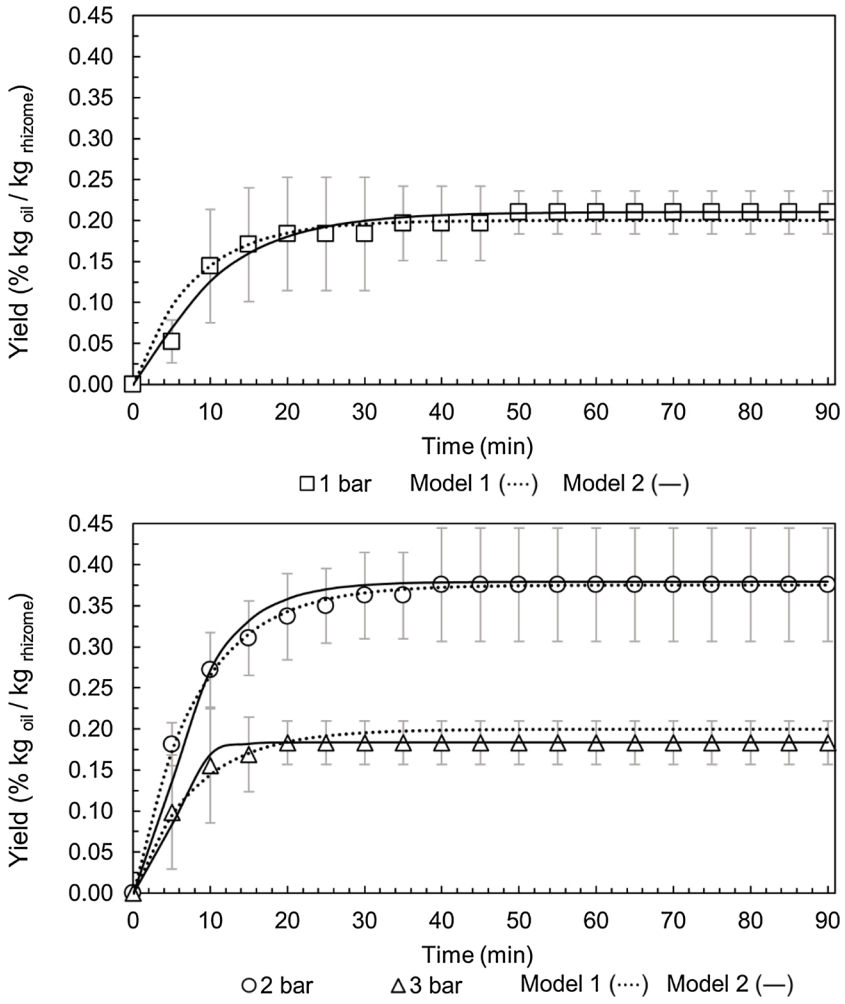

Fig. 2. Steam distillation yield for the *H. coronarium* essential oil extracted at 1, 2, and 3 bar: markers for experimental data and continuous lines for mathematical model 1 (····) and 2 (–).

Table 3
Fitted parameters by the mathematical model 1 for the steam distillation process of *H. coronarium* rhizomes.

Pressure	D.10^{11} (m^2/s)	k_c. 10^7 (m^2/s)	R^2	SSE	RMSE
1 bar	1.89	0.985	0.9173	0.0236	0.0373
2 bar	2.75	1.73	0.9979	0.0016	0.0097
3 bar	1.90	1.65	0.9018	0.0174	0.0320

Table 4
Fitted parameters by the mathematical model 2 for the steam distillation process of *H. coronarium* rhizomes.

Pressure	k_{TM} 10^3 (1/s)	K 10^5 (m^3/kg)	R^2	SSE	RMSE
1 bar	1.72	1.32	0.9768	0.0014	0.0090
2 bar	2.73	5.86	0.9754	0.0039	0.0152
3 bar	6.85	1.14	0.9835	0.0006	0.0060

2.4. Mathematical modeling

Two models were used for the mathematical representation of the extraction process. The first model, named model 1, is based on the solution presented by Crank (1975) for Fick's second law, which considers the diffusion in a slab (single particle), with solute transport on the external surface occurring by convection and equilibrium at the surface. This model describes the whole bed behavior from a single particle perspective and is often used to obtain diffusivity data from essential oil extraction processes (Almeida et al., 2013; Vargas et al., 2013; Xavier, 2016). The model, presented in Eq. 1, has two fitted parameters, diffusivity coefficient (D) and mass transfer coefficient (k_c), which were estimated by the least-square method using the Nelder-Mead Simplex method (Lagarias et al., 1998), implemented in the Matlab optimization toolbox®.

$$\frac{M_t}{M_\infty} = 1 - \sum_{n=1}^{\infty} \frac{2L^2 \exp\left(-\frac{\beta_n^2 Dt}{l^2}\right)}{\beta_n^2\left(\beta_n^2 + L^2 + L\right)} \quad (1)$$

Where t is the extraction time, M_t is the extracted mass at a given time, M_∞ is the mass in the infinite instant, l is the plant semi-thickness an β_n are the positive roots of Eq. 2.

$$\beta_n \tan\beta_n = L \quad (2)$$

$$L = \frac{lk_c}{D} \quad (3)$$

The second model, named model 2, was based on the model developed by Reverchon (1997). The model consists of one-dimensional mass balance for the extract (pseudo-component), assuming the hypothesis that a linear behavior is adequate for the solid-fluid phase equilibrium, that the solvent density and flow rate are constant along the bed, neglecting axial dispersion and considering that the supercritical fluid

Table 5
GC–MS analysis of *H. coronarium* essential oil extracted by steam distillation.

Compounds	RI[c,b]	RI_t[c]	1 bar essential oil composition (%)[a]	2 bar essential oil composition (%)[a]	3 bar essential oil composition (%)[a]
Tricyclene	917	921	0.08 ± 0.07	0.05 ± 0.08	0.08 ± 0.07
α-tujene	921	924	0.57 ± 0.07	0.59 ± 0.08	0.59 ± 0.12
α-pinene	928	932	17.59 ± 0.67	20.09 ± 1.2	19.63 ± 2.37
Camphene	941	946	1.71 ± 0.16	1.69 ± 0.19	1.71 ± 0.21
Sabinene	969	969	1.41 ± 0.12	1.59 ± 0.12	0.68 ± 0.60
β-pinene	974	974	34.1 ± 1.04	35.81 ± 0.51	35.31 ± 4.57
Myrcene	989	988	1.23 ± 0.15	1.12 ± 0.01	1.16 ± 0.02
α-phellandrene	1002	1004	2.14 ± 0.22	1.94 ± 0.07	2.21 ± 0.08
δ-3-carene	1008	1008	0.26 ± 0.01	0.08 ± 0.15	0.28 ± 0.01
α-terpinene	1015	1014	0.39 ± 0.11	0.37 ± 0.09	0.63 ± 0.06
p-cymene	1023	1022	1.21 ± 0.18	1.13 ± 0.22	1.51 ± 0.05
Limonene	1027	1024	2.46 ± 2.20	4.14 ± 0.11	3.24 ± 2.82
Eucalyptol	1030	1026	22.08 ± 5.02	19.84 ± 2.28	17.03 ± 4.85
γ-terpinene	1057	1054	1.49 ± 0.09	1.42 ± 0.10	1.95 ± 0.11
Terpinene	1086	1086	0.48 ± 0.03	0.44 ± 0.06	0.8 ± 0.29
Linalool	1100	1095	1.51 ± 0.31	1.56 ± 0.17	1.05 ± 0.44
Borneol	1163	1165	1.53 ± 0.38	1.5 ± 0.31	0.95 ± 0.40
Terpine-4-ol	1175	1174	1.99 ± 0.27	1.97 ± 0.26	1.21 ± 0.44
α-terpineol	1188	1186	0.8 ± 0.13	0.87 ± 0.15	0.6 ± 0.39
β-caryophyllene	1414	1417	1.15 ± 0.46	1.11 ± 0.22	2.06 ± 0.67
α-humulene	1449	1452	0.2 ± 0.05	0.08 ± 0.13	0.37 ± 0.25
β-bisabolene	1579	1505	0.53 ± 0.35	0.23 ± 0.20	0.23 ± 0.24
Germacrene B	1627	1559	0.37 ± 0.21	0.07 ± 0.12	0.12 ± 0.10
Caryophyllene oxide	1666	1582	0.25 ± 0.10	1.04 ± 0.51	0.37 ± 0.33
Coronarin-E	–	2132	2.29 ± 2.08	1.28 ± 0.32	3.44 ± 2.48

[a] Percentage area of each peak in relation to the chromatogram total area. The values presented are the averages of the triplicates.
[b] Calculated retention index (RI_c) in relation to a series of alkanes (C8-C20) in a HP-5MS column (30 m × 0.25 mm × 0.25 μm).
[c] Theoretical retention index (RI_t) in the HP-5MS series (Adams, 2007).

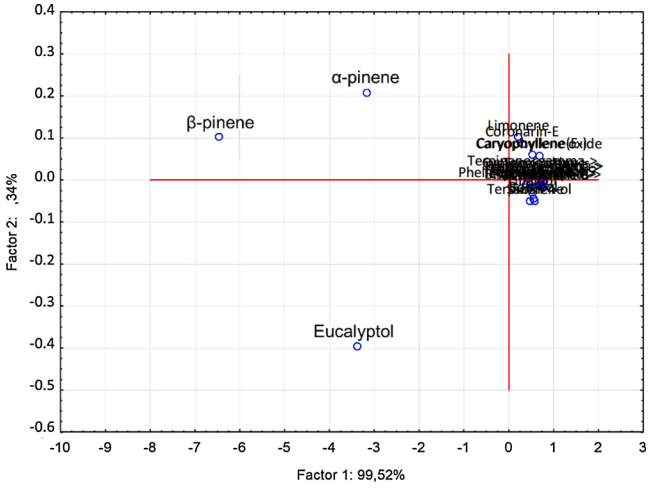

Fig. 3. Variance behavior of *H. coronarium* essential oil composition.

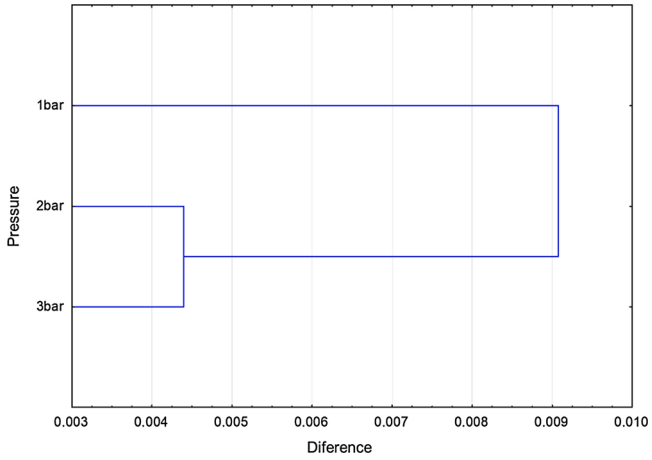

Fig. 4. Dendrogram for oils obtained from 1, 2, and 3 bar. The y-axis represents the oils obtained at the different pressures and the x-axis corresponds to 1-Pearson.

extraction is mainly controlled by internal mass transfer resistance (Falcão et al., 2017; Reverchon, 1996; Rossa et al., 2018). The mass balance is given by Eqs. 4 and 5.

Fluid phase mass balance:

$$\frac{\partial C(z,t)}{\partial t} = -\upsilon\frac{\partial C(z,t)}{\partial z} - \frac{1-\varepsilon}{\varepsilon}\rho_s\frac{\partial q(z,t)}{\partial t} \quad (4)$$

Mass balance in the solid phase:

$$\frac{\partial q(z,t)}{\partial t} = -k_{TM}[q(z,t) - K\bullet C(z,t)] \quad (5)$$

where $C(z,t)$ is the extract concentration in the vapor phase and $q(z,t)$ is its concentration in the plant; υ is the interstitial fluid velocity; ε is the porosity of the bed; k_{TM} is the internal mass transfer coefficient; ρ_s is the specific mass of the plant and where K is the equilibrium constant between the phases. The model also considers some initial and boundary conditions: $q(z,0) = q_0$ and $C(z,0) = 0$, q_0 is defined by the total amount of extract contained in the solid phase and the $C(z,0) = 0$ as a boundary condition. The linear comportment for solid-fluid phase equilibrium is expressed by $q^*(z,t) = K.C(z,t)$.

This model has been used in the literature both to represent supercritical extraction (Devi and Khanam, 2019; Reverchon, 1996; Silva et al., 2015; Vargas et al., 2006) and to simulate extraction by steam distillation (Garcez et al., 2020; Pires et al., 2019). In this model, the system of partial differential equations is solved numerically using the dynamic simulator EMSO (Environment for Modeling, Simulation, and Optimization), which is an equation-oriented simulator suitable for dynamic simulations (de P. Soares and Secchi, 2003). The internal mass transfer coefficient k_{TM}, and the equilibrium constant K, were estimated by the least-squares method and the objective function was minimized by the Nelder-Mead algorithm. The evaluation of the models was performed by determining the sum of squared errors (SSE) and the

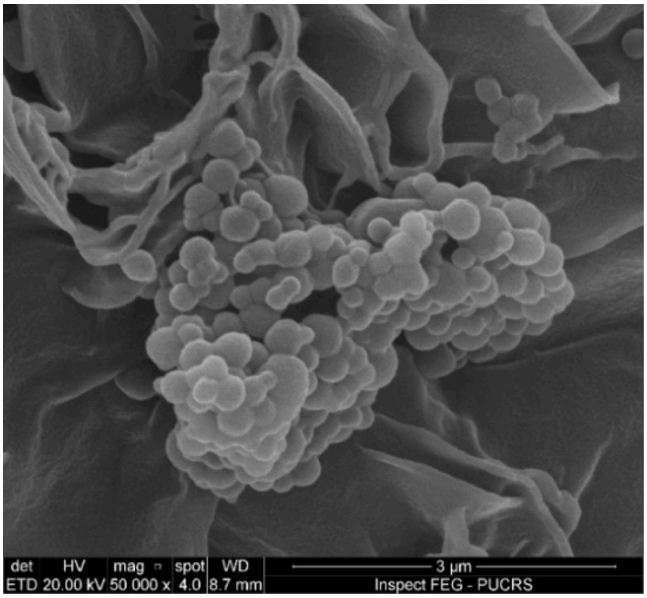

Fig. 5. Morphology of particles containing *H. coronarium* essential oil obtained by field emission scanning electron microscopy (SEM-FEG).

root-mean-square error (RMSE).

2.5. Essential oil chemical analysis

The chemical composition analysis of the essential oil was performed on a gas chromatograph (GC) model 7890A, coupled to a mass spectrometer (MS) model 5975C, both Hewlett Packard–Agilent systems. The essential oil samples were diluted in cyclohexane in the ratio of 1:10 (v/v). The column used was an HP-5MS (30 m x 25 mm, 0.25 µm). The carrier gas used was ultrapure helium with 0.8 mL/min flow, injector temperature 250 °C. The analysis method starts at a temperature of 60 °C, which is maintained for 8 min, increasing at 3 °C/min to 180 °C, holds it for 1 min, increasing at 20 °C/min to 250 °C and maintaining this temperature for 10 min. The interface temperature between GC and MS was 230 ° C, the ionization voltage was 70 eV and the mass range analyzed was 40–450 u. The split used was 1:55 and the volume injected 1 µL. The compounds were identified through their retention indexes, determined from a series of alkanes (C_8-C_{20}), with those reported in the literature (Adams, 2007) and with the comparison of mass spectra. All analyses were performed in triplicate. The chemical composition statistical analysis of essential oils was performed by the PCA method (Principal Component Analysis) to statistically evaluate the pressure process effect. The software used to perform this analysis was STATISTICA *7.1*.

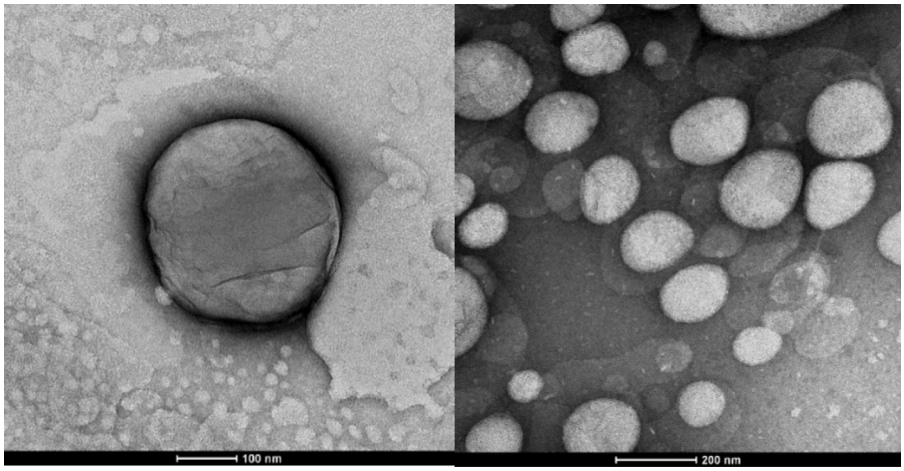

Fig. 6. Morphology of particles containing *H. coronarium* oil obtained by transmission electron microscopy (TEM) with approximation of 100 nm (left) and 200 nm (right).

Table 6
Results of dynamic light scattering analysis (DLS) for the formulations of PCL nanoparticles containing *H. coronarium* essential oil.

Formulation	Particle size (nm)	CV (%)	PdI	CV (%)	ZP (mV)	CV (%)
111	164.10 ± 0.40 [a]	2	0.163 ± 0.008 [a]	5	−37.30 ± 2.36 [a]	6
112	182.20 ± 0.82 [b]	1	0.239 ± 0.014 [b]	6	−21.40 ± 5.03 [b]	23
113	177.43 ± 1.18 [b]	1	0.182 ± 0.007 [a, c]	4	−32.67 ± 1.58 [a]	5
114	205.00 ± 2 .79 [c]	2	0.208 ± 0.012 [c, d]	6	−35.10 ± 1.01 [a]	3
115	191.30 ± 4.41 [d]	1	0.180 ± 0.012 [a, d]	7	−22.13 ± 1.79 [b]	8
211	168.33 ± 3.66 [a,b]	2	0.182 ± 0.014 [a,b]	8	−41.60 ± 7.01 [a]	17
212	170.40 ± 0.96 [a,b]	1	0.200 ± 0.007 [a,b]	3	−39.83 ± 8.91 [a]	22
213	159.50 ± 1.70 [c]	1	0.111 ± 0.002 [c]	2	−47.95 ± 3.61 [b]	8
214	163.63 ± 1.95 [a,c]	1	0.140 ± 0.032 [a,c]	23	−40.20 ± 6.95 [a]	17
215	176.97 ± 1.51 [d]	1	0.210 ± 0.019 [a,b]	9	−38.17 ± 5.84 [a]	15
311	231.60 ± 2.72 [a]	1	0.208 ± 0.021 [a]	10	−24.93 ± 2.28 [a]	9
312	185.27 ± 2.58 [b]	1	0.198 ± 0.010 [a]	5	−26.67 ± 3.58 [a]	13
313	245.53 ± 8.00 [c]	3	0.204 ± 0.038 [a]	19	*Unstable*	–
314	174.63 ± 1.40 [b]	1	0.163 ± 0.014 [a]	9	−38.77 ± 2.31 [b]	6
315	183.47 ± 4.31[b]	2	0.201 ± 0.025 [a]	8	29.71 ± 2.53 [a]	15

Values with equal superscript values do not present significant difference ($p < 0.05$).

Table 7
DLS analysis for the best nanoparticle formulation (213), corresponding nanoemulsion (E213) and polymer particles without oil (PP).

Formulation	Particle size (nm)	CV (%)	PdI	CV (%)	ZP (mV)	CV (%)
213	159.50 ± 1.697 [a]	1	0.112 ± 0.002[a]	2	−47.95 ± 3.61[a]	8
PP	187.50 ± 1.253 [a]	1	0.243 ± 0.008[b]	9	−28.07 ± 2.01[b]	7
E213	271.07 ± 22.43 [b]	8	0.401 ± 0.055[c]	14	−31.87 ± 4.28[a]	11

Values with equal superscript values show no significant difference ($p<0.05$).

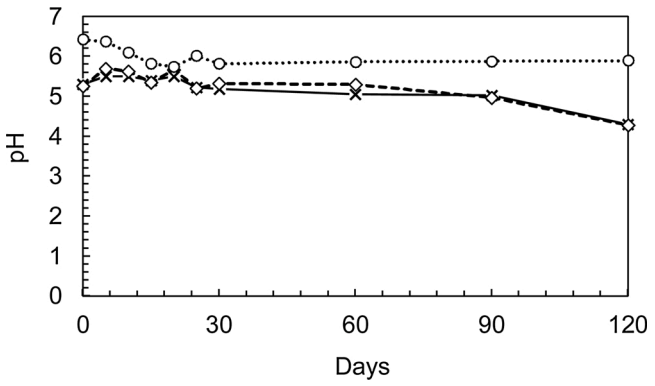

Fig. 7. pH monitoring of *H. coronarium* oil nanocapsules formulation (-x-), nanoemulsion (-◇-), and PCL particles without oil (-○-).

Table 8
Efficiency of the oil encapsulation process in PCL nanoparticles.

Formulation	Compound	% mass in emulsion	% in filtrate	Encapsulation efficiency (%)
213/E213	α-pinene	38	–	≥38
	β-pinene	70	–	≥70
	Eucalyptol	16	–	≥16
	β-caryophyllene	2	Detectable	2 < %<100

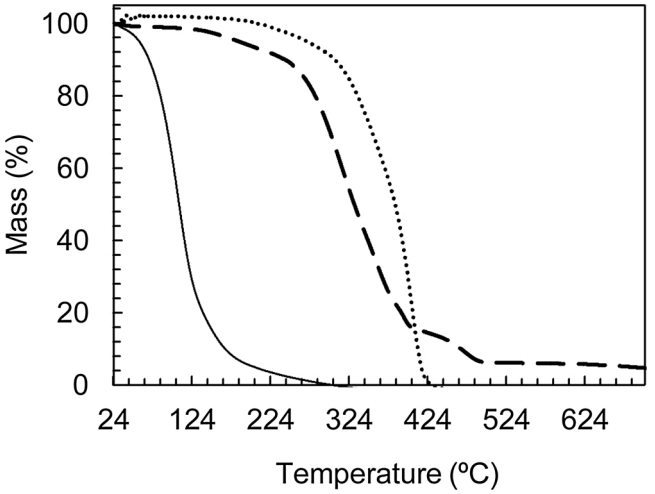

Fig. 8. TGA curves for the *H. coronarium* oil nanocapsules formulation (– – –), *H. coronarium* essential oil (—) and PCL particles (····).

2.6. Preparation of nanoformulations

The nanocapsules were prepared by nanoprecipitation, according to the method proposed by Fessi et al. (1989) with some adaptations. For this, the polycaprolactone encapsulating agent, or PCL and 0.016 g Span® 60 were diluted in 10 mL of acetone, together with the essential oil in different mass proportions of polymer/essential oil (Table 1), forming an organic phase (OP). Subsequently, the OP was added drop by drop at 10 mL of an aqueous solution containing Tween 80 0.16 % (w/w), under strong vortex agitation. The vortex supplies energy to the mixture and promotes the maximum phase dispersion possible. Afterward, the organic solvent (acetone) was removed from the solution in a rotary evaporator under reduced pressure and a constant temperature of 35 °C.

A formulation containing only the polymer (PP), without adding any oil, was prepared as a reference. The prepared nanocapsules were stored at 25 °C and all experiments were performed in triplicate. Nanoemulsions were also prepared as a reference, using the same methodology for the production of nanocapsules, excluding the PCL from the formulation.

2.7. Characterization of nanoformulations

The reproducibility of the characterization results was evaluated by calculating the coefficient of variation (CV), defined by the standard deviation ratio with the mean of the results obtained. All experiments were carried out in triplicate and their results presented as the mean of the values ± the standard deviation. The results were submitted to variance analysis (ANOVA) and Tukey test ($p < 0.05$), using Matlab 14 (MATLAB and Statistics Toolbox Release 2014a, The MathWorks, Inc., Natick, Massachusetts, United States). After the nanocapsules characterization, the best formulation was chosen to continue the experiments.

2.7.1. DLS, zeta potential, polydispersity index and pH

Nanocapsules and nanoemulsions were characterized by hydrodynamic diameter determination with dynamic light scattering technique (DLS), zeta potential (ZP), and polydispersity index (PdI), using a ZetaSizer® Nanoseries (Malvern, England) equipment. Also, nanocapsules and nanoemulsions pH were monitored over 2 and 4 months, respectively, using a digital pH meter (BEL engineering).

2.7.2. FESEM and TEM of nanocapsules

The characterization of nanocapsules was also performed by field emission scanning electron microscopy (FESEM) and transmission electron microscopy (TEM). The FESEM was performed on the Fei® Inspect F50 equipment. For imaging, one drop of each sample was applied to a carbon tape and metalized for 80 s, using gold sputtering equipment. For particle visualization, a working distance of 12 mm, radius force of 20 kV, and magnification of 2500–5000 times were used. TEM analyses were performed on Zeiss Axio Imager equipment. For these analyses, 0.1 mL of the formulations were diluted in 1 mL of Milli-Q water® and uranyl acetate (2% m/v) was used as a contrast.

2.7.3. Thermogravimetric analysis

The nanocapsules were also submitted to thermogravimetric analysis (TGA) in STD-Q600 equipment (TA Instruments, New Castle, DE), to corroborate the inclusion of oils in the polymer. For this analysis, aliquots of 5 mL of the formulations were lyophilized and 1 mg of the resulting powder was heated from 25 °C to 800 °C at the heating rate of 10 °C/min and maintained at the final temperature for 3 min (Mohamed et al., 2008). Samples of 1 mg of the oils were also submitted to this same analysis, as well as the lyophilized polymer (PP_{lio}), used as reference.

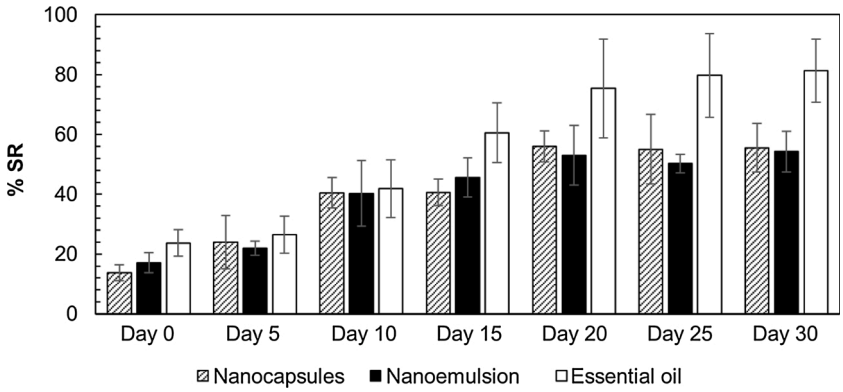

Fig. 9. DPPH radical scavenging assay with the *H. coronarium* essential oil nanocapsules formulation (crosshatch), nanoemulsion (black) and free essential oil (white).

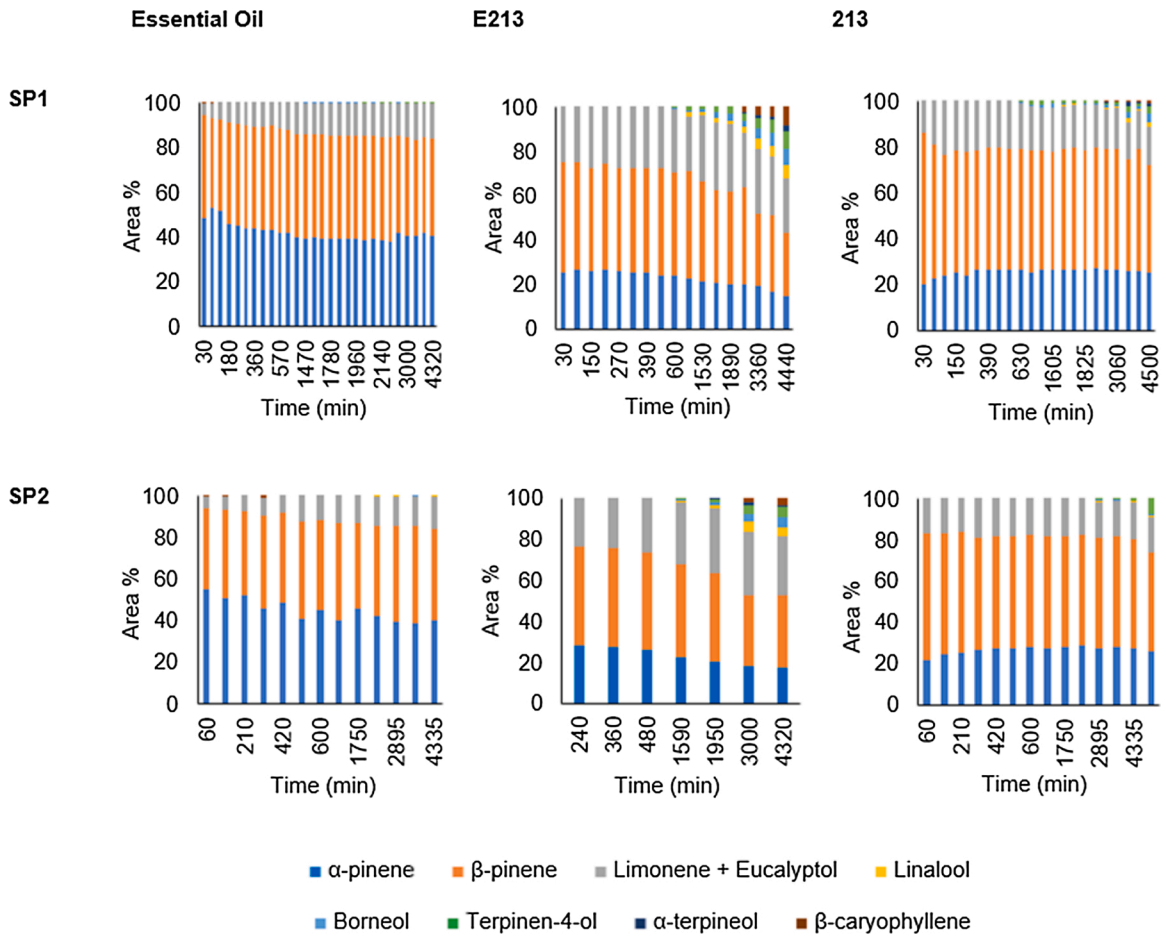

Fig. 10. Comparison of the headspace composition of pure oil, nanoemulsion (E213), and nanoparticles (213) containing essential oil at the bottom sampling ports.

2.8. Encapsulation efficiency

The essential oil mass lost in the process was evaluated since the solvent removal step occurs at reduced pressure, which may lead to the volatilization of terpenic compounds. First, aliquots of 1 mL were filtered in PTFE filters with a 0.22 μm opening, to evaluate the free essential oil in the suspension (not encapsulated). The nanocapsules suspension, nanoemulsions, and the filtrate were submitted to liquid-liquid extraction with dichloromethane and 1 μL of the organic phase was injected into the chromatograph, to quantify the amount of essential oil present in each one of them.

The method of analysis starts at a temperature of 60 °C, which is maintained for 4 min, increasing at 20 °C/min up to 250 °C and hold for 2 min. The samples were diluted in hexane and the split used was 1:55. Calibration curves using α-pinene, β-pinene, eucalyptol, and β-caryophyllene were built to quantify the compounds.

The encapsulation efficiency (Scopel et al., 2020; Zhou et al., 2019; Zili et al., 2005) determined by Eq. 6, was calculated for the major compounds α-pinene, β-pinene, and eucalyptol since the low mass percentage of minor compounds could interfere in their quantification due to the high relative experimental error.

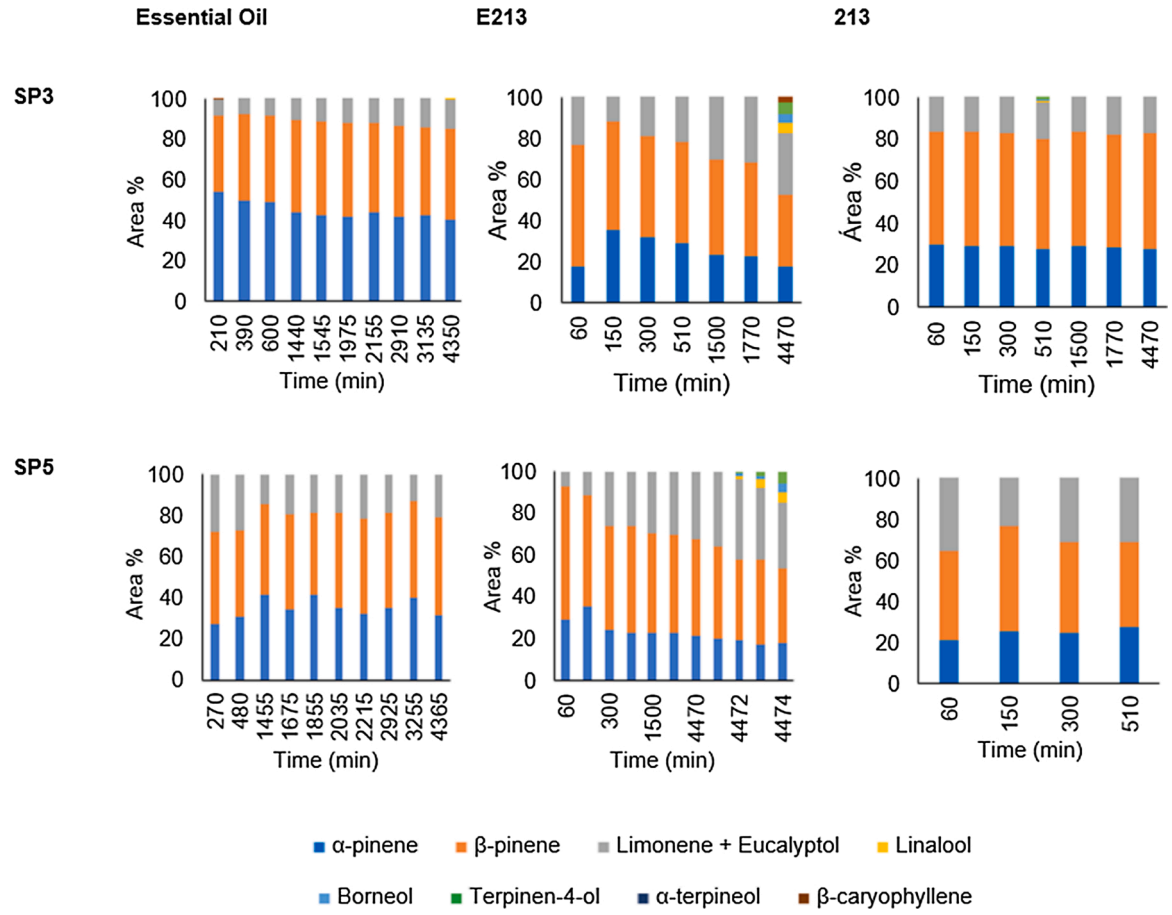

Fig. 11. Comparison of the headspace composition of pure oil, nanoemulsion (E213), and nanoparticles (213) containing essential oil at the top sampling ports.

Table 9
Parameters from the modeling of the experimental data using Peppas equation for the formulations containing *H. coronarium* and pure essential oil.

Formulation	Compounds	n	k (min^{-n})	R^2	SSE	RMSE
Nanoemulsion	α-pinene	0.37	0.0437	0.9397	0.1846	0.1074
	β-pinene	0.39	0.0392	0.9452	0.1743	0.1044
	Eucalyptol	0.41	0.0317	0.9515	0.1512	0.0972
Nanocapsules	α-pinene	0.60	0.0066	0.9861	0.0355	0.0487
	β-pinene	0.54	0.0111	0.9838	0.0363	0.1633
	Eucalyptol	0.57	0.0084	0.9851	0.0424	0.1952
Essential Oil	α-pinene	0.53	0.0123	0.9715	0.0572	0.0598
	β-pinene	0.53	0.0121	0.9680	0.0682	0.0653
	Eucalyptol	0.62	0.0055	0.9784	0.0412	0.0507

$$EE\% = \frac{m_{if} - m_{uf}}{m_{i0}} * 100 \quad (6)$$

where m_{i0} is the mass of the compound initially added, m_{if} is the mass of the compound in the suspension of nanoparticles formed and m_{uf} is relative to the compound mass present in the filtrate.

2.9. Antioxidant activity

The antioxidant activity of nanoparticles and nanoemulsions was determined by the DPPH method (Brand-Williams et al., 1995; Rufino et al., 2007), based on the capture of the DPPH radical (2,2-diphenyl-1-picryl-hydrazyl). In this method, antioxidant compounds capture the DPPH radical, producing a decrease in absorbance of a 60 μM DPPH solution, changing the color of the solution from purple to light yellow. The absorbances were read in a Biospectro SP-220 spectrophotometer, at a wavelength of 515 nm, in glass cuvettes and evaluated for a month.

On the first day (day zero) the samples were evaluated after 1 h and 2 h from the beginning of the reaction. Subsequently, the absorbances were read every 5 days. In all readings, the 60 μM DPPH solution had its absorbance measured, as blank. A DPPH scavenging percentage (%SR) is also presented in Eq. 7.

$$\%SR = \left[\left(\frac{ABS_{control} - ABS_{sample}}{ABS_{control}}\right)\right] * 100 \quad (7)$$

where ABS_{sample} is the read absorbance of the sample, either nanoparticle or nanoemulsion, and ABS_{sample} refers to the absorbance of the control formulation, being the absorbance of the PP formulation the control for the nanoparticles, and the absorbance of the pure DPPH for the nanoemulsions.

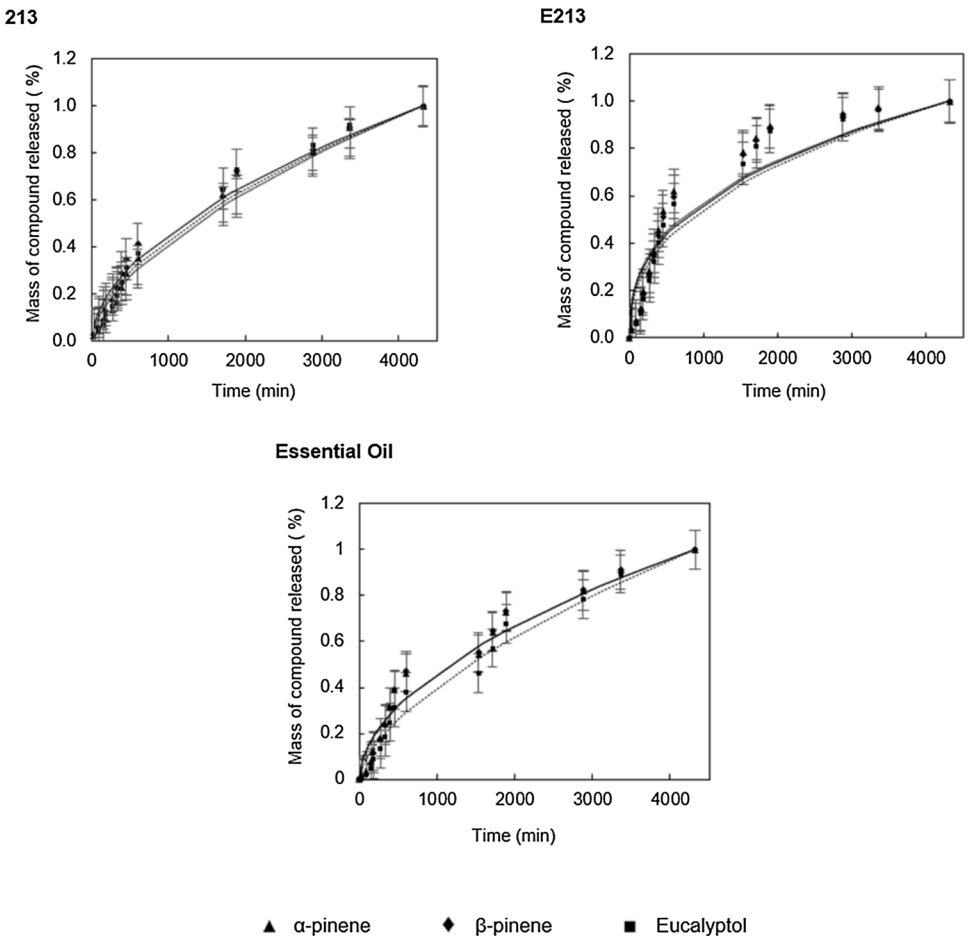

Fig. 12. Peppas analytical model fitted to the experimental release data of α-pinene (····), β-pinene (—), and eucalyptol (– – –).

2.10. Release and diffusion

The release and diffusion experiments were carried out in a Stefan tube similar to that described by Pereira et al. (2018). The diffusion tube is 2 m long and has sampling ports (SP) with PTFE septa at different distances from the tube base where the sample is located (gas-liquid interface), and it was kept in an environment with a controlled temperature of 25 °C. The SP heights and the whole apparatus are presented in Fig. 1, and the diffusion profile of the volatile compounds present in the formulations was outlined through sampling over 4 days. The fan at the top of the tube drags the air at the point where z = 2000 mm, which makes the headspace concentration at that point null. It is also considered that the surrounding air does not dissolve in the liquid mixture, there is no convection and there are no significant intermolecular interactions between the gaseous molecules of the fragrances and the surrounding air (ideal gas).

For these experiments, 5 mL of the formulations were placed in a glass container coupled at the bottom of the diffusion tube where z = 0 mm. For the diffusion analysis of pure essential oils, 1 mL of each oil was used. The headspace samples, 100 μL, were collected with a gastight syringe and analyzed by gas chromatography, on the same equipment with the same conditions used to determine the efficiency of nanoencapsulation with injections performed in splitless mode. Calibration curves were built from the headspace composition of essential oil standard major compounds. For calibration, samples of 1 mL of pure components were prepared in 20 mL vials. After 24 h to establish equilibrium, headspace samples were withdrawn by manual sampling. The data were collected in triplicate, maintaining a controlled temperature of 25 °C and varying the injection split from 5 to 400.

The mathematical modeling of the headspace data collected at the first sampling port (SP1) was performed using the Peppas (1985) equation.

$$\frac{M_t}{M_\infty} = kt^n \tag{8}$$

where M_t is the accumulated mass in a given time and M_∞ is the mass in infinite time, is time. This model presents two adjustable parameters, *k* incorporates structural and geometric effects, and the kinetic order (n), which were estimated by the least-square method using the Nelder-Mead Simplex method (Lagarias et al., 1998), implemented in the Matlab optimization toolbox®.

3. Results and discussion

3.1. Essential oil extraction and modeling

The *Hedychium coronarium* essential oil was extracted in the pilot unit by steam distillation. Fresh plant material presented 78 ± 2.7 % moisture, the specific mass of the dry plant was 1.121 ± 0.017 g/cm^3 and the particle thickness was 0.14 ± 0.02 mm. The first evaluation, regarding the amount of plant material used in the process, has not presented statistically significant differences in the extractions yields. In the extraction with 2 kg, it was observed channeling in the extractor bed, and the extractions with 0.5 kg presented the opposite behavior, the bed was dragged, presenting rhizome particles in the oil collector. The extractions with 1 kg have not presented any of these problems, which was the mass chosen for the extraction processes in the three different absolute pressures, whose yields on a dry basis and specific

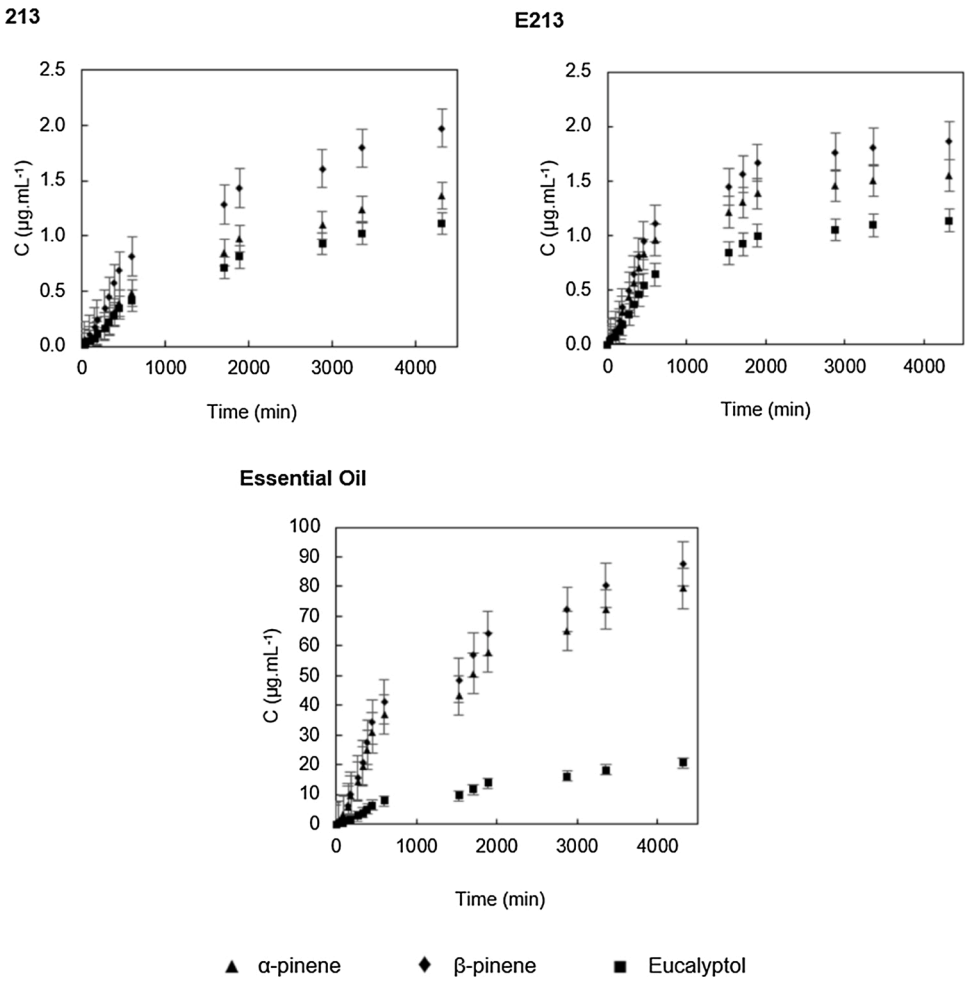

Fig. 13. Headspace concentration profile for the main compounds in nanoemulsion and nanoparticles containing *H. coronarium* oil and pure oil in the SP1.

masses are presented in Table 2. A variance analysis was applied to the mean yield results of the extractive process for the three different pressures, with a significance of 95 %, where the null hypothesis was accepted, *i.e.*, there is no significant difference between the mean yields.

The oils presented different physical characteristics, the oil obtained at 1 bar was colorless, the oil obtained at 2 bar slightly yellowish, and the 3 bar presented a stronger yellowish color. Fig. 2 presents the extraction experimental data along with the fitted models.

The estimated parameters are presented in Tables 3 and 4, as well as the determination coefficients (R^2), the sum of squares error (SSE), and the root-mean-square error (RMSE).

The results obtained by model 1 for the effective diffusion coefficient have an order of magnitude of 10^{-11} for the pressures considered, such an order of magnitude coincides with the results of Cassel et al. (2009) for the extraction of rosemary, basil, lavender essential oils as well as it agrees with the findings of Malaka et al. (2017) for the extraction of *Siphonochilus aethiopicus* essential oil by steam distillation.

From model 2, the mass transfer and the volumetric partition coefficients are obtained for the experiments conducted at 1, 2, and 3 bar. For the mass transfer coefficients, the order of magnitude found was 10^{-3}, a value that is in accordance with the order of magnitude obtained by Romdhane and Tizaoui (2005) for these coefficients in the steam distillation experiments of *Pimpinella anisum* conducted at 140 kPa and 200 kPa, when converted to the same unit used in this work. The volumetric partition coefficient values have an order of magnitude of 10^{-5}, which coincides with the order of magnitude found by Rossa et al. (2018) for the extraction of the essential oil of *Piper hispidinervum*. The RMSE determination, a measure of the difference between the values predicted by the model and the experimental values, produces values very close to zero for the results of models 1 and 2, which indicates the accuracy of the models used to represent the phenomenon physical transfer of mass.

3.2. Essential oil chemical analysis

The essential oil compounds identification, by GC–MS, is presented in Table 5. Unidentified compounds were omitted and correspond to 2.18 % of the total area detected. The oils have three major compounds: β-pinene (>34.10 %), α-pinene (>17.59 %), and eucalyptol (>17.03 %), these components were also reported as the majority by Ray et al. (2018b) for populations of *H. coronarium* collected from different locations of Eastern India and by Joy et al. (2007).

Through the chemical composition statistical analysis performed using the PCA method, it was observed that three compounds stood out from the others, α-pinene, β-pinene, and eucalyptol. This behavior was already expected since these compounds are the majority and that the covariance of these with the other compounds is large. This behavior can be observed in Fig. 3.

These variations, however, are not significant when comparing the essential oils extracted at each different condition, as can be seen in Fig. 4. The dendrogram presents the distances between oils as 1-Pearson. Pearson's coefficient is a similarity measure between data, this means that the percentage of similarity between oils obtained at 2 bar and 3 bar is 99.57 % and can be grouped in a cluster that is similar to the oil obtained at 1 bar in more than 99.1 %. Thus, in terms of chemical composition, the oils obtained in the three different conditions are

statistically similar.

3.3. Characterization and encapsulation efficiency

The particles produced presented a spherical and homogeneous morphology, according to the FESEM images (Fig. 5).

The morphology was confirmed by transmission electron microscopy (TEM) analysis, whose images are presented in Fig. 6, with an approximation of 100 nm, on the left, in a single particle, and approximation of 200 nm, on the right.

The hydrodynamic diameter analysis of the nanocapsules, as well as the polydispersity index and zeta potential, are presented in Table 6. The different formulations are coded regarding the three different pressure conditions and the five different PCL/oil ratios.

Presenting lower particle size, lower PdI, zeta potential lower than -30 mV, and low levels of variance, formulations 111, 213, and 314 were chosen to continue with the tests. Statistically, there was no difference between the particle sizes of these three samples. Sample 213 presented lower PdI and stronger anionic zeta potential, therefore was chosen as the best formulation. The comparison between sample 213, a formulation containing only the polymer without adding any oil (PP), and a nanoemulsion, coded as E213 is presented in Table 7.

Sample E213 presented a larger particle diameter than the corresponding nanoparticle formulation. The high polydispersity index (>0.1) also indicates a low homogeneity of the sample size distribution.

Regarding the pH of the three formulations evaluated, it remained stable until the 90th day, when it presented a slight fall, except for the PP solution as shown in Fig. 7. Nanocapsules, nanoemulsions, and PCL particles all showed a slightly acidic character, which follows previously reported data for formulations containing PCL and various drugs (Külkamp-Guerreiro et al., 2009).

The pH maintenance of the formulations also indicates that there is no significant polymer degradation, which had been previously reported for periods of up to 8 months (Guterres et al., 1995; Lemoine et al., 1996). This is an indication that the oil remains encapsulated since the formulations containing free oil present lower pH values than the nanocapsules formulations. The decrease in the pH value seems to be directly related to the stability of the nanoemulsion since both formulations presented very similar behaviors and that within this period the polymer remains stable.

Table 8 presents the remaining mass percentages at the end of the process, regarding the initial mass used for the formulation, for the selected compounds. It was considered that all oil retained in the nanoemulsion was successfully encapsulated since most of the compounds were not detected in the filtrate analysis of the nanoparticle formulation. This efficiency can then be higher than the remaining percentage in the emulsion since the polymer protects the oil during the rotary evaporation process.

Other compounds detected in nanoemulsion E213 were limonene, borneol, terpinene-4-ol, α-terpinene, and β-caryophyllene. In the filtrate analysis of formulation 213, the only detectable compound was β-caryophyllene, which presents a lower affinity with the polymer used in this work.

The thermogravimetric analysis results are presented in Fig. 8, as the mass loss percentage curve *versus* temperature.

As expected, the PCL nanoparticles increased the thermal stability of the oils. The pure essential oil presented degradation in the range of 74 °C–174 °C, while the nanocapsules presented three stages of degradation from 124 °C to 474 °C. The first stage may be due to free oil evaporation from 124 °C to 250 °C, the second stage of 274 °C–400 °C seems to be associated with PCL degradation. The third stage, from 400 °C to 474 °C indicates the complete degradation of the polymer. The pure polymer degradation curve has a single stage that starts at 224 °C and ends at 455 °C with the total degradation of the polymer.

3.4. Antioxidant activity of formulations

Initially, the DPPH reaction was monitored for a period of 55 days, but after the 30th day, the DPPH solution became highly unstable due to the free radical natural degradation, reflected in the high experimental reading errors. The formulations were compared with the same mass of free essential oil.

The free essential oil presented high scavenging activity in the zero-day reading, higher than the activity of formulations 213 and E213. This result can be observed in Fig. 9.

The DDPH scavenging of the two formulations remained around 50 % during the 30 days. The free essential oil continued to act for 15 days reaching its maximum scavenging capacity on the 20th day. These results can be confirmed in Fig. 9. Both formulations, with and without polymer, seem to promote a controlled release of antioxidant compounds.

The expansion of bioavailability revealed by the permanence of the antioxidant effect in releases from encapsulated structures was also observed by Weisany et al., 2019 by studying the release of active principles from essential oil of *Anethum graveolens* L. and *Thymus daenensis* L. encapsulated in silver nanoparticles designed to exert antimicrobial action against plant diseases.

The DPPH scavenging analysis confirms the controlled release of oil compounds from nanoemulsions and nanoparticles, as well as demonstrates the capacity of these formulations to protect the system core from the free radical oxidative action. Any future application would benefit from the robustness and prolonged stability of the formulations.

3.5. Diffusion and modeling

The diffusion profiles from the formulations containing *H. coronarium* oil and the pure oil obtained in the diffusion tube at different distances from the source are presented in Figs. 10 and 11. Regarding the composition profile, the headspace of formulations containing the essential oil did not present such an evident variation between the nanoemulsion and the nanoparticles, as well as for the pure essential oil. The major compounds identified in the pure essential oil are α-pinene (>17.59 %), β-pinene (>34.10 %), and eucalyptol (>17.03 %), and these are also the compounds that make up the majority of the gaseous phase. Among them, eucalyptol is the heaviest compound, with 154.25 g/gmol and the less volatile, which agrees with a slightly increased contribution to the profile compared to other compounds at longer times. The addition of the polymer wall resulted in a constant release profile for a longer period, which is of great interest for the formulation of aroma products, since it is desirable that the aroma not only has a prolonged duration, but its organoleptic characteristics do not change significantly. This same profile can be observed in the release of pure oil, which means that the formulation containing PCL will have the same sensory behavior as pure oil, with the advantage of release it in smaller amounts, promoted by the polymeric wall, which will extend the diffusion of these compounds.

Table 9 presents the parameters obtained from the modeling of the experimental data using the Peppas (1985).

The release profile for each major compound was built to evaluate its kinetics, following the Peppas model approach (Fig. 12). The n values found for the release of the compounds present in the nanoemulsion were lower than 0.43, characteristic value for Fickian diffusion (Siepmann and Siepmann, 2013). The n values for the compounds released from the nanoparticles were in the region of anomalous transport ($0.43 < n < 0.85$). This anomalous transport may be associated with other release mechanisms such as tumescence and/or polymer matrix erosion (Scopel et al., 2020).

The coefficients k are the diffusive kinetics constants, it incorporates structural and geometric effects, and the estimated values ratify that the addition of PCL to the formulation resulted in a delay in the release of α-pinene, β-pinene, and eucalyptol when compared to the

nanoemulsion.

Although the percentage mass release for each of the three compounds presented a very similar profile (Fig. 12), both for nanoemulsion and nanocapsules, the concentration of compounds in the air was quite distinct and is presented in Fig. 13.

From Fig. 13, the headspace concentration reaches the steady-state after 3000 min. The same does not occur for the nanoparticles release, which only reaches the same final concentration of the nanoemulsion after 4000 min. The pure essential oil presents much higher concentrations than the corresponding in the formulations and did not reach the steady-state after 4320 min of analysis for the pinenes. Only eucalyptol reached steady-state with a final concentration of 20.5 μg/mL, almost 20 times higher than the maximum concentration of 1.1 μg/mL in the formulations.

4. Conclusions

The chemical composition analysis of essential oil obtained by steam distillation of *Hedychium coronarium* rhizomes was performed in CG-MS and the major compounds were identified as β-pinene (>34.10 %), α-pinene (>17.59 %), and eucalyptol (>17.03 %). The mathematical models adjusted from the experimental extraction yield curves presented a good fit to the experimental data, and parameters associated with the mass transfer phenomenon in the extraction process were obtained. These parameters can be used in future stages of scale change for industrial processes. Nanoemulsions and nanoparticles containing essential oil were successfully obtained and characterized. The best polymer/oil ratio was 1:3, which presented nanocapsules with an average particle diameter of 159 nm, PdI of 0.122, and zeta potential of -47.95. The analysis by FESEM and TEM confirmed the spherical morphology of the obtained particles. The pH of the formulations was stable for a period of 90 days and the antioxidant activity analysis showed that the formulations continued to react with the free radical for a period of 30 days, while the free oils reached their maximum %SR on the 20th day. The headspace profile of the formulations was monitored for 4 days and its behavior is visibly affected by the type of formulation. Nanoemulsions presented profiles more similar to the release of compounds from pure oils, while nanoparticles were more affected by the encapsulation efficiency and compound/polymer interaction. The mathematical modeling with the Peppas model indicated that for all formulations, the release occurred by non-Fickian mechanisms (anomalous transport), the diffusion is occurring simultaneously with other release mechanisms, such as polymer degradation and tumescence.

CRediT authorship contribution statement

Caroline F. da Silva: Conceptualization, Methodology, Validation, Formal analysis, Investigation, Writing - review & editing. **Rafaela R. Petró:** Methodology, Validation, Investigation, Writing - original draft, Visualization. **Rafael N. Almeida:** Formal analysis, Data curation, Writing - original draft, Visualization. **Eduardo Cassel:** Resources, Writing - review & editing, Funding acquisition. **Rubem M.F. Vargas:** Resources, Writing - review & editing, Supervision, Project administration, Funding acquisition.

Declaration of Competing Interest

The authors report no declarations of interest.

Acknowledgements

This work was supported by the CNPq, National Council of Scientific and Technological Development, CAPES, Coordination of Superior Level Staff Improvement and FAPERGS, Research Support Foundation of the State of Rio Grande do Sul.

References

Adams, R.P., 2007. Identification of Essential Oils by Gas chromatography/mass Spectrometry. Carol Stream Allured Publ. Corp.

Ali, S., Sotheeswaran, S., Tuiwawa, M., Smith, R.M., 2002. Comparison of the composition of the essential oils of Alpinia and Hedychium species—essential oils of Fijian plants, part 1. J. Essent. Oil Res. 14, 409–411.

Almeida, R.N., Neto, R.G., Barros, F.M.C., Cassel, E., von Poser, G.L., Vargas, R.M.F., 2013. Supercritical extraction of Hypericum caprifoliatum using carbon dioxide and ethanol+ water as co-solvent. Chem. Eng. Process. Process Intensif. 70, 95–102.

Beck, R., Guterres, S., Pohlmann, A., 2011. Nanocosmetics and Nanomedicines, New Approaches for Skin Care. Springer Berlin Heidelberg, Berlin, Heidelberg. https://doi.org/10.1007/978-3-642-19792-5.

Brand-Williams, W., Cuvelier, M.-E., Berset, C., 1995. Use of a free radical method to evaluate antioxidant activity. LWT-Food Sci. Technol. 28, 25–30.

Caldas, G.F.R., da Silva Oliveira, A.R., Araújo, A.V., Lafayette, S.S.L., Albuquerque, G.S., da Costa Silva-Neto, J., Costa-Silva, J.H., Ferreira, F., da Costa, J.G.M., Wanderley, A.G., 2015. Gastroprotective mechanisms of the monoterpene 1, 8-cineole (eucalyptol). PLoS One 10, e0134558.

Cassel, E., Vargas, R.M.F., Martinez, N., Lorenzo, D., Dellacassa, E., 2009. Steam distillation modeling for essential oil extraction process. Ind. Crops Prod. 29, 171–176.

Castangia, I., Manca, M.L., Caddeo, C., Maxia, A., Murgia, S., Pons, R., Demurtas, D., Pando, D., Falconieri, D., Peris, J.E., Fadda, A.M., Manconi, M., 2015. Faceted phospholipid vesicles tailored for the delivery of Santolina insularis essential oil to the skin. Colloids Surf. B Biointerfaces 132, 185–193. https://doi.org/10.1016/j.colsurfb.2015.05.025.

Chan, E.W.C., Wong, S.K., 2015. Phytochemistry and pharmacology of ornamental gingers, Hedychium coronarium and Alpinia purpurata: a review. J. Integr. Med. 13, 368–379.

Crank, J., 1975. The Mathematics of Diffusion. Oxford Sci. Publ, UK, p. 414. https://doi.org/10.1016/0306-4549(77)90072-X.

de P. Soares, R., Secchi, A.R., 2003. EMSO: a new environment for modelling, simulation and optimisation. Comput. Aided Chem. Eng. 14, 947–952.

de Souza Junior, E.T., Siqueira, L.M., Almeida, R.N., Lucas, A.M., Silva, C.G.Fda, Cassel, E., Vargas, R.M.F., 2020. Comparison of different extraction techniques of Zingiber officinale essential oil. Braz. Arch. Biol. Technol. 63.

Devi, V., Khanam, S., 2019. Development of generalized and simplified models for supercritical fluid extraction: case study of papaya (Carica papaya) seed oil. Chem. Eng. Res. Des. 150, 341–358.

dos Santos, B.C.B., Barata, L.E.S., Marques, F.A., Baroni, A.C.M., Karnos, B.A.C., de Oliveira, P.R., Guerrero Jr, P.G., 2010. Composition of leaf and rhizome essential oils of Hedychium coronarium Koen. From Brazil. J. Essent. Oil Res. 22, 305–306.

El Asbahani, A., Miladi, K., Badri, W., Sala, M., Addi, E.H.A., Casabianca, H., El Mousadik, A., Hartmann, D., Jilale, A., Renaud, F.N.R., 2015. Essential oils: from extraction to encapsulation. Int. J. Pharm. 483, 220–243.

Ezhilarasi, P.N., Karthik, P., Chhanwal, N., Anandharamakrishnan, C., 2013. Nanoencapsulation techniques for food bioactive components: a review. Food Bioprocess Technol. 6, 628–647. https://doi.org/10.1007/s11947-012-0944-0.

Falcão, M.A., Fianco, A.L.B., Lucas, A.M., Pereira, M.A.A., Torres, F.C., Vargas, R.M.F., Cassel, E., 2012. Determination of antibacterial activity of vacuum distillation fractions of lemongrass essential oil. Phytochem. Rev. 11, 405–412.

Falcão, M.A., Scopel, R., Almeida, R.N., do Espirito Santo, A.T., Franceschini, G., Garcez, J.J., Vargas, R.M.F., Cassel, E., 2017. Supercritical fluid extraction of vinblastine from Catharanthus roseus. J. Supercrit. Fluids 129, 9–15.

Fessi, H., Puisieux, F., Devissaguet, J.P., Ammoury, N., Benita, S., 1989. Nanocapsule formation by interfacial polymer deposition following solvent displacement. Int. J. Pharm. 55, R1–R4.

Garcez, J.J., da Silva, C.G.F., Lucas, A.M., Fianco, A.L., Almeida, R.N., Cassel, E., Vargas, R.M.F., 2020. Evaluation of different extraction techniques in the processing of Anethum graveolens L. seeds for phytochemicals recovery. J. Appl. Res. Med. Aromat. Plants 18, 100263.

Guterres, S.S., Fessi, H., Barratt, G., Devissaguet, J.-P., Puisieux, F., 1995. Poly (DL-lactide) nanocapsules containing diclofenac: I. Formulation and stability study. Int. J. Pharm. 113, 57–63. https://doi.org/10.1016/0378-5173(94)00177-7.

Hartati, R., Suganda, A.G., Fidrianny, I., 2014. Botanical, phytochemical and pharmacological properties of Hedychium (Zingiberaceae)–A review. Procedia Chem. 13, 150–163.

Joy, B., Rajan, A., Abraham, E., 2007. Antimicrobial activity and chemical composition of essential oil from Hedychium coronarium. Phyther. Res. An Int. J. Devoted to Pharmacol. Toxicol. Eval. Nat. Prod. Deriv. 21, 439–443.

Külkamp-Guerreiro, I.C., Paese, K., Guterres, S.S., Pohlmann, A.R., 2009. Stabilization of lipoic acid by encapsulation in polymeric nanocapsules designed for cutaneous administration. Quim. Nova 32, 2078–2084. http://hdl.handle.net/10183/72881.

Lagarias, J.C., Reeds, J.A., Wright, M.H., Wright, P.E., 1998. Convergence properties of the Nelder–Mead simplex method in low dimensions. SIAM J. Optim. 9, 112–147.

Lechat-Vahirua, I., François, P., Menut, C., Lamaty, G., Bessiere, J.-M., 1993. Aromatic plants of French Polynesia. I. Constituents of the essential oils of rhizomes of three Zingiberaceae: zingiber zerumbet Smith, Hedychium coronarium Koenig and Etlingera cevuga Smith. J. Essent. Oil Res. 5, 55–59.

Lemoine, D., Francois, C., Kedzierewicz, F., Preat, V., Hoffman, M., Maincent, P., 1996. Stability study of nanoparticles of poly(ε-caprolactone), poly(d,l-lactide) and poly(d, l-lactide-co-glycolide). Biomaterials 17, 2191–2197. https://doi.org/10.1016/0142-9612(96)00049-X.

Malaka, M.S., Naidoo, K., Kabuba, J., 2017. Extraction of Siphonochilus aethiopicus essential oil by steam distillation. Chem. Eng. Commun. 204, 813–819.

Mohamed, A., Finkenstadt, V.L., Gordon, S.H., Biresaw, G., Palmquist, D.E., Rayas-Duarte, P., 2008. Thermal properties of PCL/gluten bioblends characterized by TGA, DSC, SEM, and infrared-PAS. J. Appl. Polym. Sci. 110, 3256–3266. https://doi.org/10.1002/app.28914.

Omata, A., Yomogida, K., Teshima, Y., Nakamura, S., Hashimoto, S., Arai, T., Furukawa, K., 1991. Volatile components of ginger flowers (Hedychium coronarium Koenig). Flavour Fragr. J. 6, 217–220.

Peppas, N.A., 1985. Analysis of Fickian and non-Fickian drug release from polymers. Pharm. Acta Helv. 60, 110–111.

Pereira, J., Costa, P., Coimbra, M.C., Rodrigues, A.E., 2018. The trail of perfumes. AIChE J. 00, 1–8. https://doi.org/10.1002/aic.16155.

Piorkowski, D.T., McClements, D.J., 2014. Beverage emulsions: recent developments in formulation, production, and applications. Food Hydrocoll. 42, 5–41.

Pires, V.P., Almeida, R.N., Wagner, V.M., Lucas, A.M., Vargas, R.M.F., Cassel, E., 2019. Extraction process of the Achyrocline satureioides (Lam) DC. essential oil by steam distillation: modeling, aromatic potential and fractionation. J. Essent. Oil Res. https://doi.org/10.1080/10412905.2019.1569564.

Ray, A., Jena, S., Kar, B., Sahoo, A., Panda, P.C., Nayak, S., Mahapatra, N., 2018a. Volatile metabolite profiling of ten Hedychium species by gas chromatography mass spectrometry coupled to chemometrics. Ind. Crops Prod. 126, 135–142.

Ray, A., Jena, S., Dash, B., Kar, B., Halder, T., Chatterjee, T., Ghosh, B., Panda, P.C., Nayak, S., Mahapatra, N., 2018b. Chemical diversity, antioxidant and antimicrobial activities of the essential oils from Indian populations of *Hedychium coronarium* Koen. Ind. Crops Prod. 112, 353–362. https://doi.org/10.1016/j.indcrop.2017.12.033.

Reverchon, E., 1996. Mathematical modeling of supercritical extraction of sage oil. AIChE J. 42, 1765–1771.

Reverchon, E., 1997. Supercritical fluid extraction and fractionation of essential oils and related products. J. Supercrit. Fluids 10, 1–37. https://doi.org/10.1016/S0896-8446(97)00014-4.

Romdhane, M., Tizaoui, C., 2005. The kinetic modelling of a steam distillation unit for the extraction of aniseed (Pimpinella anisum) essential oil. J. Chem. Technol. Biotechnol. Int. Res. Process. Environ. Clean Technol. 80, 759–766.

Rossa, G.E., Almeida, R.N., Vargas, R.M.F., Cassel, E., Moyna, G., 2018. Sequential extraction methods applied to Piper hispidinervum: an improvement in the processing of natural products. Can. J. Chem. Eng. 96, 756–762. https://doi.org/10.1002/cjce.23020.

Rufino, M., Alves, R.E., de Brito, E.S., de Morais, S.M., Sampaio, C., de, G., Pérez-Jimenez, J., Saura-Calixto, F.D., 2007. Metodologia Científica: Determinação Da Atividade Antioxidante Total Em Frutas Pela Captura Do Radical Livre DPPH. Embrapa Agroindústria Trop. Técnico.

Sakhanokho, H.F., Sampson, B.J., Tabanca, N., Wedge, D.E., Demirci, B., Baser, K.H.C., Bernier, U.R., Tsikolia, M., Agramonte, N.M., Becnel, J.J., 2013. Chemical composition, antifungal and insecticidal activities of Hedychium essential oils. Molecules 18, 4308–4327.

Scopel, R., Falcão, M.A., Cappellari, A.R., Morrone, F.B., Guterres, S.S., Cassel, E., Kasko, A.M., Vargas, R.M.F., 2020. Lipid-polymer hybrid nanoparticles as a targeted drug delivery system for melanoma treatment. Int. J. Polym. Mater. Polym. Biomater. 1–12.

Siepmann, J., Siepmann, F., 2013. Mathematical modeling of drug dissolution. Int. J. Pharm. 453, 12–24.

Silva, G.F.D., Gandolfi, P.H.K., Almeida, R.N., Lucas, A.M., Cassel, E., Vargas, R.M.F., 2015. Analysis of supercritical fluid extraction of lycopodine using response surface methodology and process mathematical modeling. Chem. Eng. Res. Des. https://doi.org/10.1016/j.cherd.2015.05.039.

Teixeira, M.A., Rodriguez, O., Gomes, P., Mata, V., Rodrigues, A., 2012. Perfume Engineering: Design, Performance and Classification. Butterworth-Heinemann.

Vargas, R.M.F., Cassel, E., Gomes, G.M.F., Longhi, L.G.S., Atti-Serafini, L., Atti-Santos, A. C., 2006. Supercritical extraction of carqueja essential oil: experiments and modeling. Brazilian J. Chem. Eng. 23, 375–382.

Vargas, R.M.F., Barroso, M.S.T., Neto, R.G., Scopel, R., Falcão, M.A., Silva, C.F., Cassel, E., 2013. Natural products obtained by subcritical and supercritical fluid extraction from Achyrocline satureioides (Lam) D.C. Using CO2. Ind. Crops Prod. 50, 430–435. https://doi.org/10.1016/j.indcrop.2013.08.021.

Weisany, W., Amini, J., Samadi, S., Hossaini, S., Yousefi, S., Struik, P.C., 2019. Nano silver-encapsulation of Thymus daenensis and Anethum graveolens essential oils enhances antifungal potential against strawberry anthracnose. Ind. Crops Prod. 141, 111808 https://doi.org/10.1016/j.indcrop.2019.111808.

Xavier, V.B., 2016. Análise cromatográfica/olfatométrica do potencial aromático de extratos naturais livres e incorporados a materiais pela impregnação supercrítica, p. 160.

Xavier, V.B., Vargas, R.M.F., Minteguiaga, M., Umpiérrez, N., Dellacassa, E., Cassel, E., 2013. Evaluation of the key odorants of Baccharis anomala DC essential oil: new applications for known products. Ind. Crops Prod. 49, 492–496.

Zhou, D., Zhou, F., Ma, J., Ge, F., 2019. Microcapsulation of Ganoderma lucidum spores oil: evaluation of its fatty acids composition and enhancement of oxidative stability. Ind. Crops Prod. 131, 1–7.

Zili, Z., Sfar, S., Fessi, H., 2005. Preparation and characterization of poly-ε-caprolactone nanoparticles containing griseofulvin. Int. J. Pharm. 294, 261–267.